

Near Absence of Support Effects in Toluene Hydrogenation Catalyzed by MgO-Supported Iridium Clusters

S. E. Deutsch, F.-S. Xiao, and B. C. Gates¹

Department of Chemical Engineering and Materials Science, University of California, Davis, California 95616

Received January 8, 1997; revised May 13, 1997; accepted May 14, 1997

Iridium cluster catalysts were prepared by reaction of $[\text{Ir}_4(\text{CO})_{12}]$ with MgO that had been calcined at 300, 500, or 700°C to vary to degree of hydroxylation, followed by removal of the CO ligands from the iridium by treatment in He. The catalysts were tested for toluene hydrogenation at 60, 80, and 100°C and 1 atm. Extended X-ray absorption fine structure (EXAFS) spectra of each catalyst after 120 h of continuous operation in the absence of deactivation showed that they had changed little, if any, nearly retaining the Ir_4 tetrahedra of the precursor $[\text{Ir}_4(\text{CO})_{12}]$. The catalyst with the most highly hydroxylated support (calcined at 300°C) evidently underwent slight aggregation, giving iridium clusters with nuclearities of about 6 ± 2 . Thus the data allow a determination of the influence of the degree of hydroxylation of the support on the catalytic activity in the near absence of metal cluster size effects. The turnover frequency at 60°C decreased from 7.5×10^{-4} to $6.2 \times 10^{-4} \text{ s}^{-1}$ as the MgO calcination temperature increased from 300 to 700°C. The change is negligible in view of the experimental errors. These results, combined with similar values of the turnover frequency for toluene hydrogenation catalyzed by $\gamma\text{-Al}_2\text{O}_3$ -supported clusters that were also nearly Ir_4 , indicate that the effects of changes in nonreducible metal oxide supports are very small. The Ir_4 clusters are regarded as quasi-molecular in character, with the metal oxide supports being multidentate ligands; the ligand effects are inferred to be similar for the $\gamma\text{-Al}_2\text{O}_3$ and MgO with various densities of surface O and OH groups. © 1997 Academic Press

INTRODUCTION

The term *metal-support interaction* connotes several complex phenomena in catalysis by supported metals (1), including, for example, the withdrawal of electron density from metal particles by the support (2, 3), which is believed to influence the high dehydrocyclization selectivity of Pt/LTL zeolites incorporating cations such as K^+ and Ba^{2+} (4–6). Metal-support interactions are also invoked when the support enhances catalysis by providing sites for spillover or reaction (7). The term *strong metal-support interaction* usually refers to the migration of reducible metal oxides onto supported metals to cover them partially and reduce

the chemisorption capacity and catalytic activity; however, a metal oxide that migrates onto a metal may sometimes increase the catalytic activity of the metal by acting like a promoter (1, 8–10).

The various influences of the support are not easily resolved or distinguished from other effects, such as metal particle size effects. In attempts to isolate support effects from metal particle size effects, we have prepared samples with relatively high degrees of structural uniformity, including cationic metal complexes bonded to almost irreducible metal oxide supports. For example, using surface organometallic synthesis and extended X-ray absorption fine structure (EXAFS) spectroscopy for structural characterization, Deutsch *et al.* (11) prepared mononuclear osmium carbonyls anchored to $\gamma\text{-Al}_2\text{O}_3$ by either two or three Os–O bonds, depending on the number of CO ligands bonded to the osmium (three or two, respectively). Triantafyllou *et al.* (12) used EXAFS spectroscopy to determine slight changes in metal–oxygen bond distances in a family of mononuclear rhenium carbonyls supported on MgO which had been hydroxylated or methoxylated to various degrees.

Although EXAFS results characterizing nearly molecular metal complexes on metal oxides give clear evidence of chemical bonding and structure, these samples are not representative of typical supported metal catalysts, which incorporate clusters or particles of metal rather than mononuclear metal complexes. Thus, in the work reported here, we have gone beyond metal complexes to metal clusters, proceeding from the premise that preparation of nearly uniform metal clusters on a support that is varied in its degree of hydroxylation may allow experiments to isolate the effects of the support on catalytic activity. We report structures (determined by EXAFS spectroscopy) and catalytic activities of variously hydroxylated MgO-supported samples incorporating iridium clusters that are extremely small (to maximize the metal-support interactions) and nearly uniform (to allow separation of support effects from cluster size effects). Elsewhere (13), we reported EXAFS and X-ray absorption near edge spectra (XANES) of unused catalysts, providing information about the metal-support

¹ To whom correspondence should be addressed.

interface structure and bonding and the metal oxidation state.

Toluene hydrogenation was chosen as the catalytic test reaction because it proceeds at low temperatures, helping to ensure that the clusters remain intact and the catalyst stable during the reaction, and because rates of this reaction are affected by the electronic nature of the supported metal (3, 14, 15). The adsorption of toluene on metal particles is strong because of the interaction of the delocalized π -electrons with the metal. A support effect that makes the metal particles electron deficient has been suggested to make this adsorption stronger and cause the catalytic hydrogenation reaction to proceed at a lower rate (3, 14, 15).

EXPERIMENTAL METHODS

Catalyst preparation. The catalyst preparation is described in detail elsewhere (13); only a short summary is given here. MgO powder (EM Science) was calcined under flowing O_2 for 2 h followed by vacuum for 14 h at 300, 500, or 700°C. The surface area of the MgO decreased from about 70 to about 20 m²/g as the treatment temperature increased from 300 to 700°C. In what follows, the subscript on MgO indicates the temperature of calcination, in °C. [Ir₄(CO)₁₂] (Strem) was allowed to react with the calcined MgO by slurrying in dried, degassed hexane or pentane. The resulting supported iridium carbonyl clusters were decarbonylated by treatment in flowing He (Liquid Carbonic, 99.997%) at 300°C for 2 h. Each sample contained 1.0 wt% Ir.

Catalytic hydrogenation of toluene. Toluene hydrogenation catalysis was carried out at steady state in a thermostated, once-through Pyrex flow reactor at 60, 80, or 100°C and atmospheric pressure. The catalyst particles (typically, 40 mg, but sometimes more when the experiments were intended to give used catalysts for EXAFS analysis), initially consisting of the MgO-supported iridium carbonyl clusters, were mixed with approximately 1 g of particles of inert, low-surface-area α -Al₂O₃. The mixture in the reactor was treated in flowing He at 300°C for 2 h to remove the carbonyl ligands.

Toluene (Baker) was dried and degassed by distillation over Na/benzophenone. Toluene liquid was fed by a metering pump (Isco) at a rate of 8 ml/min into a vaporizer held at 116°C, where it was mixed with H₂ formed by electrolysis of water in a Balston generator and flowing at 44 ml (NTP)/min. Products of the reaction were analyzed by on-line gas chromatography. Details of the experimental methods are given in a thesis (16).

EXAFS characterization of used catalysts. Catalysts that had been used for 120 h of continuous operation in the flow reactor were transferred to a N₂-filled glovebox without coming in contact with air, where they were unloaded and stored. Samples were sealed in vials and placed

in a desiccator for transport to the National Synchrotron Light Source, where EXAFS experiments were carried out at beamline X-11A.

Approximately 150 mg of each used catalyst was pressed into a self-supporting wafer and loaded in a N₂-filled glove box into an airtight EXAFS cell, which was cooled with liquid nitrogen. Each sample was scanned at least twice at the Ir L_{III} edge (11215 eV), and the scans were averaged. Each scan took about 15 min. The beam current was at least 110 mA, and the beam energy was 2.5 GeV. Details of the experimentation are as reported elsewhere (13, 17).

EXAFS DATA ANALYSIS

Phase shift and backscattering amplitude data were obtained from experimentally measured EXAFS spectra of suitable reference compounds. Platinum foil was used as a reference for Ir–Ir absorber-backscatterer pairs; NaPt(OH)₄ was used for Ir–O absorber-backscatterer pairs. The crystallographic data and details of the preparation of the reference files are summarized in Table 1. The transferability of phase shifts and backscattering amplitudes has been verified by experimental results (18–20).

EXAFS data were extracted from the raw X-ray absorption data by standard procedures (21). Normalization of the EXAFS data was done by dividing the absorption intensity by the height of the background absorption at 50 eV past the absorption edge. The main EXAFS contributions were isolated by Fourier filtering of the extracted EXAFS data, with k^3 weighting (k is the wave vector) (Table 2). Analysis was performed on the filtered data. Parameters were estimated by fitting by using the Koningsberger difference file technique (22) and the XDAP data analysis software (23). Low- Z and high- Z contributions were fitted both in r space (r is the radial distance from absorbing Ir atom to the backscattering atom) and in k space, with both k^1 and k^3 weighting to avoid overemphasizing the contributions of either the low- Z or high- Z backscatterers.

Details are as given elsewhere (13).

TABLE 1
Structural Parameters Characterizing the Reference Compounds Used in EXAFS Data Analysis^a

Sample	Crystallographic data			Fourier transform		
	Shell	N	R , Å	Δk , Å ⁻¹	Δr , Å	n
Pt foil	Pt–Pt	12	2.77	1.9–19.8	1.9–3.0	3
Na ₂ Pt(OH) ₆	Pt–O	6	2.05	1.4–17.7	0.5–2.0	3

^a Notation: N , coordination number for absorber-backscatterer pair; R , radial distance from absorber to backscatterer; Δk , limits used for forward Fourier transformation (k is the wave vector); Δr , limits used for inverse Fourier transformation (r is the distance); n , power of k used for Fourier transformation.

TABLE 2
Parameters Used for Fourier Filtering of EXAFS Data
Characterizing Used Catalysts^a

Support	<i>n</i>	Δk , Å ⁻¹	Δr , Å	<i>p</i>
MgO ₃₀₀	2	3.03–14.29	0.93–3.20	17.3
MgO ₅₀₀	3	2.92–14.36	1.01–3.20	16.9
MgO ₇₀₀	3	2.99–13.65	1.15–3.23	15.1

^a Notation as in Table 1, except *p*, the number of allowable free parameters in the EXAFS analysis, is estimated as $p = 2(\Delta k \Delta r / \pi) + 1$.

RESULTS

EXAFS data characterizing used catalysts. The EXAFS results characterizing the used catalysts are summarized in Table 3. The data characterizing each catalyst were fitted satisfactorily with Ir–Ir and Ir–O contributions; there was no evidence of any remaining carbonyl ligands on the iridium, confirming that the decarbonylation was complete, as expected (13).

The EXAFS data characterizing the used MgO₃₀₀-supported catalyst were fitted with two contributions, Ir–Ir and Ir–O. The overall fit of the data is shown in Figs. 1 and 2. The Ir–Ir contribution (Fig. 3) is characterized by a coordination number of 3.7 and a distance of 2.70 Å. The Ir–O contribution (Fig. 4) is characterized by a coordination number of 3.6 and a distance of 2.59 Å.

A good fit of the EXAFS data characterizing the used MgO₅₀₀-supported catalyst required three contributions, an Ir–Ir and two Ir–O contributions. The Ir–Ir contribution is characterized by a coordination number of 3.0 and a distance of 2.65 Å. The longer Ir–O contribution is characterized by a coordination number of 1.0 and a distance of

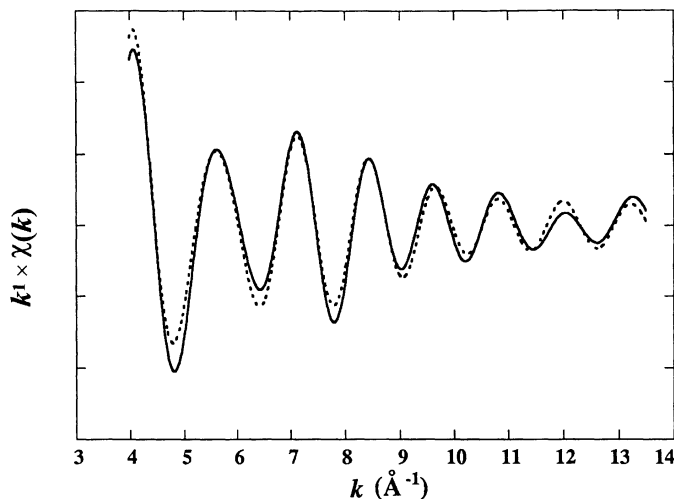


FIG. 1. Filtered EXAFS data characterizing the Ir₄/MgO₃₀₀ sample after use for toluene hydrogenation (solid line) and the sum of the best-fit calculated Ir–Ir and Ir–O contributions (dashed line).

2.55 Å. The shorter Ir–O contribution is characterized by a coordination number of 1.3 and a distance of 2.07 Å. Comparisons of the data and the fits are shown elsewhere (24).

The EXAFS data characterizing the used MgO₇₀₀-supported catalyst were also fitted well with two contributions, Ir–Ir and Ir–O. The Ir–Ir contribution is characterized by a coordination number of 2.6 and a distance of 2.68 Å. The Ir–O contribution is characterized by a coordination number of 3.5 and a distance of 2.65 Å. The data and fits are shown elsewhere (24).

Toluene hydrogenation catalysis. The catalysts were active for the hydrogenation of toluene to give

TABLE 3

Best-fit Calculated Parameters Representing EXAFS Data
Characterizing Used Catalysts^a

Support	Backscatterer	<i>N</i>	<i>R</i> , Å	$\Delta\sigma^2$, Å ²	<i>E</i> ₀ , eV
MgO ₃₀₀	Ir	3.7	2.70	0.00420	−2.44
	O	3.6	2.59	0.00713	5.59
MgO ₅₀₀	Ir	3.0	2.65	0.00316	3.73
	O	1.0	2.55	0.00110	6.70
	O	1.3	2.07	0.00110	0.00
MgO ₇₀₀	Ir	2.6	2.68	0.00365	2.80
	O	3.5	2.65	0.01000	−0.40

^a Notation: *N*, average Ir-backscatterer coordination number; *R*, radial distance from Ir to backscatterer; $\Delta\sigma^2$, Debye–Waller factor; *E*₀, inner potential correction. The estimated error bounds are as follows: *N*, ±15%; *R*, ±2%; $\Delta\sigma^2$, ±10%; and *E*₀, ±10%.

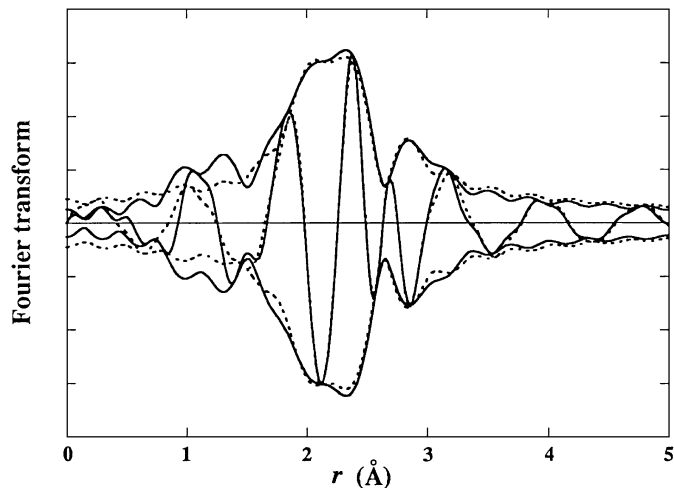


FIG. 2. k^1 -Weighted Fourier transform ($4.0 < k < 13.5$ Å^{−1}) of the filtered EXAFS data characterizing the used Ir₄/MgO₃₀₀ sample (solid line) and the sum of the best-fit calculated Ir–Ir and Ir–O contributions (dashed line).

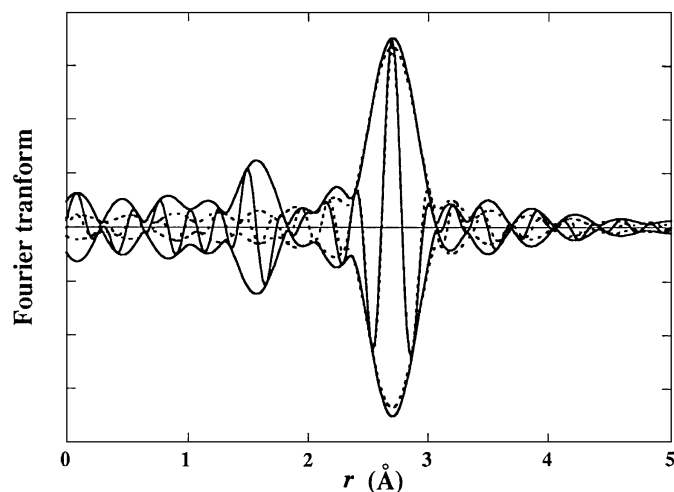


FIG. 3. k^3 -Weighted Fourier transform ($4.0 < k < 13.5 \text{ \AA}^{-1}$, phase- and amplitude-corrected on the basis of platinum foil reference data) of the filtered EXAFS data characterizing the used $\text{Ir}_4/\text{MgO}_{300}$ catalyst minus the best-fit calculated Ir–O contribution (solid line) and the best-fit calculated Ir–Ir contribution (dashed line).

methylcyclohexane; no side products were observed. After a short induction period, each catalyst was stable, as indicated by the lack of detectable changes in the conversion as a function of time on stream; data are similar to those reported for $\gamma\text{-Al}_2\text{O}_3$ -supported iridium clusters (17). The conversions were low and differential, determining reaction rates directly, as before (17).

Turnover frequencies were estimated from the reaction rates on the basis of the EXAFS results indicating extremely small iridium clusters and dispersions of unity. The

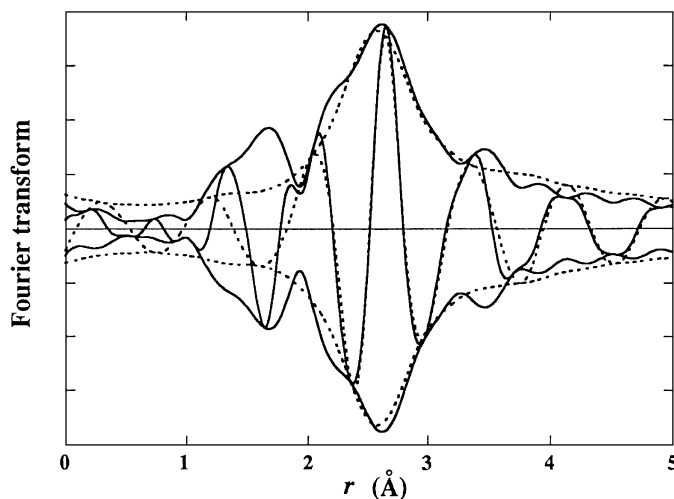


FIG. 4. k^1 -Weighted Fourier transform ($4.0 < k < 12.0 \text{ \AA}^{-1}$, phase-corrected on the basis of Pt–O reference data) of the filtered EXAFS data characterizing the used $\text{Ir}_4/\text{MgO}_{300}$ catalyst minus the calculated Ir–Ir contribution (solid line) and the best-fit calculated Ir–O contribution (dashed line).

TABLE 4

Turnover Frequencies Characterizing Metal Oxide-Supported Cluster Catalysts Modeled as Ir_4

Support	$10^3 \times$ Turnover frequency at 60°C , s^{-1a}	$10^3 \times$ Turnover frequency at 80°C , s^{-1}	$10^3 \times$ Turnover frequency at 100°C , s^{-1}	Ref.
MgO_{300}	0.75 ± 0.04	2.5	6.3	This work
MgO_{500}	0.70 ± 0.04	1.9	5.6	This work
MgO_{700}	0.62 ± 0.03	1.6	3.7	This work
MgO_{400}	0.63			(25)
$\gamma\text{-Al}_2\text{O}_3$	0.94			(25)
$\gamma\text{-Al}_2\text{O}_3$	1.6			(26)

^a Each error bound represents a precision, indicated by the reproducibility of repeat experiments determined with catalyst samples from a particular batch; these precisions do not represent uncertainties associated with catalyst preparation.

implicit assumption that all the iridium atoms were accessible is flawed because any blockage of access to iridium atoms by the support is neglected; more information about the structure of the metal–support interface would be needed to account for any such blockage. The turnover frequencies are summarized in Table 4; they indicate barely any difference from one catalyst to another.

DISCUSSION

Structures of fresh and used catalysts. The EXAFS data characterizing the MgO -supported iridium clusters following decarbonylation of the supported iridium carbonyl precursor in He at 300°C for 2 h (and prior to use as a catalyst) indicate Ir–Ir first-shell coordination numbers of approximately 3, consistent with the presence of Ir_4 tetrahedra. Details of the structures of the supported clusters are presented elsewhere (13). These samples are part of a family of catalysts approximated as supported Ir_4 (27).

The MgO_{500} -supported catalyst, after use, was characterized by an Ir–Ir coordination number of 3.0, indicating that the tetrahedral framework of the precursor $[\text{Ir}_4(\text{CO})_{12}]$ and the fresh decarbonylated catalyst remained essentially intact during the catalysis experiment. The used MgO_{700} -supported catalyst is characterized by a first-shell Ir–Ir coordination number of 2.6 (Table 3). This value is, within the estimated experimental error of $\pm 15\text{--}20\%$, also indistinguishable from the value of 3 for a tetrahedron. No evidence of higher-shell Ir–Ir contributions was found for these samples, as would have been expected if there had been formation of larger clusters or raft-like clusters on the MgO surface. Thus, both the MgO_{500} - and MgO_{700} -supported used catalysts are modeled as approximately Ir_4/MgO . The EXAFS data are in accord with the catalyst performance data, demonstrating the stability of each of these two samples during catalysis.

The used MgO₃₀₀-supported catalyst was characterized by an Ir–Ir coordination number of 3.7 (Table 3). This result is barely distinguishable within the expected experimental error from the value of 3 characteristic of Ir₄ tetrahedra. The data indicate that this catalyst incorporated iridium clusters containing about 6 ± 2 atoms each, on average.

Thus, the data suggest that some slight aggregation of the iridium took place on the support that was most highly hydroxylated. The hydroxyl group coverages of the MgO after calcination at 300, 500, or 700°C are estimated to be about 100, 50, or 5% of a monolayer, respectively (28). (However, a conflicting report (29) leads to estimates of the hydroxyl group coverages of 40, 15, and 5% of a monolayer, respectively.) Consistent with this inference that the tendency for metal aggregation is associated with the degree of surface hydroxylation, EXAFS data characterizing MgO₃₀₀-supported iridium clusters that had been treated in H₂ at 300°C for 2 h indicate that the iridium underwent slight aggregation, forming clusters of about 10 ± 5 atoms each, on average (13). The observations are in qualitative agreement with numerous reports (e.g., 30, 31) showing that increasing surface hydroxylation and water increase rates of aggregation or sintering of supported noble metals.

In summary, the important conclusions are (1) the iridium clusters in the catalysts after use were almost unchanged in structure from the clusters that were initially present and are approximated as Ir₄ and (2) the data therefore represent the catalytic properties of the desired samples, those with supports incorporating various densities of surface OH groups and nearly the same metal cluster structures, allowing a separation of support and cluster size effects in the catalysis.

Near lack of support effect in toluene hydrogenation catalysis. The turnover frequencies summarized in Table 4 show only a weak dependence of the catalytic activity for toluene hydrogenation on the degree of hydroxylation of the MgO support. The small changes in the catalytic activity associated with changes in the support hydroxylation may be negligible in view of the likely experimental errors suggested by the comparison of results from two separate measurements of the turnover frequency for toluene hydrogenation catalyzed by γ -Al₂O₃-supported samples approximated as Ir₄ (Table 4).

A comparison of the turnover frequencies summarized in Table 4 indicates that MgO and γ -Al₂O₃ are almost indistinguishable from each other in their effects on the toluene hydrogenation activity of clusters approximated as Ir₄. These two metal oxides evidently interact similarly with the clusters (25). Regarding these supports as multidentate ligands for the clusters, as they are for mononuclear metal carbonyl complexes (11, 12, 32), we infer that the ligands provided by MgO are nearly equivalent to the ligands provided by γ -Al₂O₃ and that O and OH groups on MgO are similar

as ligands, consistent with the observations of Triantafyllou *et al.* (12) that the metal–oxygen bond distances in mononuclear rhenium carbonyls on MgO barely depend on the relative numbers of O and OH ligands provided by the MgO. The results are also in accord with infrared spectra characterizing rhenium tricarbonyls bonded to almost fully hydroxylated and almost fully dehydroxylated MgO and showing a difference of only 22 cm⁻¹ in the high-frequency metal carbonyl peak (32).

Alternatively, one might speculate that different effects of the O and OH ligands are fuzzed out by the presence of ligands formed from the reactants (such as carbonaceous deposits). However, the changes in activity of the catalysts during the initial break-in period were small, which implies that the effects of any ligands formed from the reactants were also small. Furthermore, there is no evidence of such additional ligands in the EXAFS data, but it is usually not possible to distinguish O from C backscatterers (unless, for example, they are present in linear metal–C–O moieties that lead to multiple scattering). Perhaps the indications of two Ir–O contributions in one of the EXAFS data sets and of only one such contribution in the two others could be attributed to a slight modification of the metal–support interface caused by deposits, but instead we consider it more likely that the differences represent minor differences in the EXAFS data quality in regard to the weak Ir–O contributions; the lack of a trend in the EXAFS data indicating the shorter Ir–O contribution with a decreasing degree of hydroxylation of the support lends support to this hypothesis.

Because the effects of changes in the degree of hydroxylation of the MgO support or the substitution of γ -Al₂O₃ for MgO as the support are so small for catalysis by clusters as small as Ir₄, we suggest that the effects of such changes in the supports should be negligible for clusters and particles of noble metals larger than Ir₄, which includes virtually all supported noble metals. This inference is restricted to supports that do not partially cover the metal or play another direct catalytic role.

If the apparent small influence of the degree of hydroxylation of the MgO on the catalytic activity is presumed to be significant even in view of the experimental errors, then it can be explained as a weak electronic effect. The XANES experiments reported elsewhere (13) for MgO-supported iridium clusters after treatment in helium show that the *d*-band density on the iridium atoms decreases slightly as the calcination temperature of the MgO increases. The infrared results characterizing MgO-supported iridium carbonyl clusters (13) and those characterizing mononuclear MgO-supported rhenium carbonyls (32) indicate that the MgO support becomes more electron-withdrawing as the degree of hydroxylation of the MgO increases.

Toluene hydrogenation has been suggested to be sensitive to the electronic nature of the supported metal

catalysts, as toluene bonds strongly to the metal (14). Tri *et al.* (14) reported that the adsorption of toluene on zeolite-supported platinum increased and the rate of toluene hydrogenation decreased as the platinum became more electron deficient. Phuong *et al.* (15) reported that the adsorption of toluene on silica-supported Group 8 metal increased with decreasing *d*-electron density of the metal. (Lin and Vannice (7, 33) reported that the turnover frequency for arene hydrogenation catalyzed by supported platinum particles is sensitive to the type of support, with the activity of Pt/SiO₂-Al₂O₃ being greater than that of Pt/SiO₂, but the activity advantage of the more acidic support was attributed to adsorption of arene on the support near the platinum particles, where it reacted with hydrogen on the platinum.)

The electron withdrawing nature of the MgO support may therefore be expected to have some (small) influence on the activity of MgO-supported iridium clusters. MgO₇₀₀ is a strong Brønsted base, containing both Lewis acid and Lewis base sites (34). The XANES results characterizing the fresh catalyst (13) show that MgO₇₀₀ has a stronger electron-withdrawing capability than MgO calcined at lower temperatures. Thus electron-deficient iridium clusters on MgO₇₀₀ might be expected to adsorb toluene more strongly than iridium clusters on the other MgO supports, leading to the relatively low rate of toluene hydrogenation on the sample with the most highly dehydroxylated support.

In summary, the small changes in the electronic nature of the MgO-supported iridium clusters observed in the XANES and infrared spectra could be related to the small changes in turnover frequency for toluene hydrogenation. As the MgO calcination temperature increases, the support becomes more electron-withdrawing, the supported iridium clusters become more electron-deficient, forming stronger π -bonds with adsorbed toluene and lowering the rate of hydrogenation of the adsorbed toluene. However, we reemphasize that the suggested effects may be negligibly small and that the differences in activity from one catalyst to another may be only a reflection of experimental errors.

Iridium cluster size effects in toluene hydrogenation (25, 35, 36). The effects of iridium cluster size in toluene hydrogenation have been investigated with samples initially incorporating γ -Al₂O₃-supported Ir₄ that had been treated in H₂ at various temperatures for various times to cause aggregation of the iridium to various degrees. The data show that the cluster size effects are significant, with the turnover frequency increasing by 1–2 orders of magnitude as the cluster nuclearity increased from four to roughly 100, on average (35). Evidently, the pattern of structure insensitivity does not extend to clusters smaller than about 10 Å in diameter (25, 35); the results presented here strongly suggest that these cluster size effects were not confused with support effects, although the various treatment conditions used to

cause cluster aggregation no doubt led to changes in the relative number of O and OH ligands on the γ -Al₂O₃ surface.

CONCLUSIONS

Clusters of approximately four iridium atoms each were prepared on MgO supports with varying degrees of hydroxylation and used as catalysts for toluene hydrogenation. The clusters nearly retained their original nuclearities of four on each of the supports after 120 h on stream in a flow reactor, although the EXAFS data suggest a slight aggregation of the clusters on the MgO that had been calcined at only 300°C. The turnover frequency for toluene hydrogenation decreased from $7.5 \times 10^{-4} \text{ s}^{-1}$ for the MgO₃₀₀-supported catalyst to $6.2 \times 10^{-4} \text{ s}^{-1}$ for the MgO₇₀₀-supported catalyst, but the difference is negligible in view of the experimental errors. If the small variation in activity is considered to be significant, it might be explained as an indication of metal-support interactions which lower the electron density of the iridium clusters as the degree of support dehydroxylation increases.

ACKNOWLEDGMENTS

The research was supported by the U.S. Department of Energy, Office of Energy Research, Office of Basic Energy Sciences, Division of Chemical Sciences, contract number FG02-87ER13790. We acknowledge the support of the U.S. Department of Energy, Division of Materials Sciences, under Contract No. DE-FG05-89ER45384, for its role in the operation and development of beam line X-11A at the National Synchrotron Light Source (NSLS). The NSLS is supported by the Department of Energy, Division of Materials Sciences and Division of Chemical Sciences, under Contract No. DE-AC02-76CH00016. We thank the staff of beam line X-11A for their assistance. The X-ray absorption data were analyzed with the XDAP software (23).

REFERENCES

1. Stevenson, S. A., Dumesic, J. A., Baker, R. T. K., and Ruckenstein, E., Eds., "Metal-Support Interactions in Catalysis, Sintering, and Redispersion." Van Nostrand Reinhold, New York, 1987.
2. Samant, M. G., and Boudart, M., *J. Phys. Chem.* **95**, 4070 (1991).
3. Larsen, G., and Haller, G. L., *Catal. Lett.* **3**, 103 (1989).
4. Besoukhanova, C., Guidot, J., and Barthomeuf, D., *J. Chem. Soc. Faraday Trans. 1* **77**, 1595 (1981).
5. Triantafyllou, N. D., Deutsch, S. E., Alexeev, O., Miller, J. T., and Gates, B. C., *J. Catal.* **159**, 14 (1996).
6. Tamm, P. W., Mohr, D. H., and Wilson, C. R., in "Catalysis 1987" (J. W. Ward, Ed.), p. 335. Elsevier, Amsterdam, 1988.
7. Lin, S. D., and Vannice, M. A., *J. Catal.* **143**, 539 (1993).
8. Tauster, S. J., Fung, S. C., and Garten, R. L., *J. Am. Chem. Soc.* **100**, 170 (1978).
9. Tauster, S. J., and Fung, S. C., *J. Catal.* **55**, 29 (1978).
10. Tauster, S. J., and Steger, J. J., *Mat. Res. Soc. Symp. Proc.* **111**, 419 (1988).
11. Deutsch, S. E., Chang, J.-R., and Gates, B. C., *Langmuir* **9**, 1284 (1993).
12. Triantafyllou, N. D., Purnell, S. K., Papile, C. J., Chang, J.-R., and Gates, B. C., *Langmuir* **10**, 4077 (1994).
13. Deutsch, S. E., Mestl, G., Knözinger, H., and Gates, B. C., *J. Phys. Chem. B* **101**, 1374 (1997).

14. Tri, T. M., Massardier, J., Gallezot, P., and Imelik, B., in "Metal-Support and Metal-Additive Effects in Catalysis" (B. Imelik, C. Naccache, G. Coudurier, H. Praliaud, P. Meriaudeau, P. Gallezot, G. A. Martin, and J. C. Vedrine, Eds.), p. 141. Elsevier, Amsterdam, 1982.
15. Phoung, T. T., Massardier, F., and Gallezot, P., *J. Catal.* **102**, 456 (1986).
16. Xu, Z., Ph.D. Dissertation, University of Delaware, Newark, DE, 1994.
17. Zhao, A., and Gates, B. C., *J. Am. Chem. Soc.* **118**, 2458 (1996).
18. van Zon, F. B. M., Maloney, S. D., Gates, B. C., and Koningsberger, D. C., *J. Am. Chem. Soc.* **115**, 10317 (1993).
19. Kawi, S., Chang, J.-R., and Gates, B. C., *J. Phys. Chem.* **97**, 5375 (1993).
20. Kampers, F. W. H., and Koningsberger, D. C., *Faraday Discuss. Chem. Soc.* **89**, 137 (1990).
21. Kampers, F. W. H., Thesis, University of Eindhoven, The Netherlands, 1988.
22. Koningsberger, D. C., in "Synchrotron Techniques in Interfacial Electrochemistry" (C. A. Melendres and A. Tadjeddine, Eds.), p. 181. Kluwer, Alphen an den Rijn, The Netherlands, 1994.
23. Vaarkamp, M., Linders, J. C., and Koningsberger, D. C., *Physica B* **209**, 159 (1995).
24. Deutsch, S. E., Ph.D. Dissertation, University of Delaware, Newark, DE, 1995.
25. Xu, Z., Xiao, F.-S., Purnell, S. K., Alexeev, O., Kawi, S., Deutsch, S. E., and Gates, B. C., *Nature (London)* **372**, 346 (1994).
26. Zhao, A., and Gates, B. C., *J. Catal.* **168**, 60 (1997).
27. Gates, B. C., *Chem. Rev.* **95**, 511 (1995).
28. Anderson, P. J., Horlock, R. F., and Oliver, J. F., *Trans. Faraday, Soc.* **61**, 2754 (1965).
29. Dunski, H., Jozwiak, W. K., and Sugier, H., *J. Catal.* **146**, 166 (1994).
30. Ruckenstein, E., and Hu, X. D., *J. Catal.* **100**, 1 (1986).
31. Triantafillou, N. D., and Gates, B. C., *J. Phys. Chem.* **98**, 8431 (1994).
32. Papile, C. J., and Gates, B. C., *Langmuir* **8**, 74 (1992).
33. Lin, S. D., and Vannice, M. A., *J. Catal.* **143**, 554 (1993).
34. Stair, P. C., *J. Am. Chem. Soc.* **104**, 4044 (1982).
35. Xiao, F.-S., Weber, W. A., Alexeev, O., and Gates, B. C., "Proceedings, 11th International Congress Catalysis," part B, 1996, p. 1135.
36. Gates, B. C., in "Catalysis by Di- and Polynuclear Metal Cluster Complexes" (F. A. Cotton and R. D. Adams, Eds.), VCH, Weinheim, in press.